TECNIACÚSTICA
CUENCA 2023

AEROACOUSTICS SIMULATION OF TALGO'S RUNNING GEAR FRAME "RODAL"

Ana Vieira[1*], *Ph.D.*

[1]Departamento de Innovación, Patentes Talgo SL

RESUMEN

Los trenes Talgo son fácilmente reconocibles debido a su sistema de rodadura independiente y guiada (conocido como rodal). Esta característica permite un numero de soluciones difíciles de implementar en trenes tradicionales, por ejemplo, coches a nivel de andén y un sistema automático de cambio de ancho de vía. La rodadura, en cualquier vehículo ferroviario, impacta directamente el ruido de paso de un tren, debido a su contribución al ruido de rodadura y aerodinámico. Este artículo presenta una metodología computacional para el cálculo del ruido aerodinámico generado a alta-velocidad en la zona ubicada entre dos coches (paso entre coches). El cálculo del ruido aerodinámico es realizado en dos pasos: un análisis de dinámica de fluidos computacional para determinar el campo de velocidad y presión del dominio, seguido por un análisis MEF (Métodos de los Elementos Finitos) basado en la analogía de Lighthill. Los resultados son presentados para el punto de certificación de ruido de paso como definido en la *ISO EN 3095:2013: "Measurement of noise emitted by railbound vehicles".*

Palabras Clave— ferrovía, ruido aerodinámico, ruido de paso.

ABSTRACT

Talgo trains are immediately recognizable due to their single-axle running gears with independently rotating wheels (a system known as *rodal*). This characteristic type of running gear facilitates a number of solutions that are difficult to implement in conventional rolling stock, such as a coach floor at the platform level and an automatic variable gauge system. The rolling stock has a direct influence on the train pass-by noise due to its contribution both to rolling and aerodynamic noise. This paper presents a computational procedure to calculate the aerodynamic noise generated at high speed by an inter-coach gap with a *rodal*. The aerodynamic noise is calculated in two steps: a CFD (Computational Fluid Dynamics) analysis to determine the velocity and pressure fields of the domain followed by a FEM (Finite Element Method) simulation of the flow-induced noise based on the Lighthill's acoustic analogy. Results are presented for observer positions specified in the ISO EN 3095:2013: "*Measurement of noise emitted by railbound vehicles*".

Keywords— railway, aerodynamic noise, pass-by noise.

1. INTRODUCTION

Rail transport plays an important role in the decarbonization of the economy [1], as it has a significantly lower carbon footprint compared to other modes of transport. This great advantage, together with other benefits, such as lower operational costs and reliability, contributes to the continuous growth of the rail market [2]

The expansion of rail transport raises concerns about noise pollution, as studies have shown a direct relation between noise exposure and health issues such as high blood pressure, headache, and sleep disturbances [3].

Regulators are setting progressively more restrictive noise limits to protect communities from excessive noise levels. Mitigation measures, such as noise barriers and night curfews can be effective [4], but they are also costly. Reducing the noise source is therefore the preferable solution.

The noise produced by a passing train is a combination of rolling and aerodynamic noise, being the latter considered predominant for an operational velocity higher than 300 km/h [5].

Aerodynamic noise is generated by the interaction of an unsteady flow and a solid body. The sound power of aerodynamic noise sources increases at a rate of the 6^{th}-8^{th} power of the flow speed [6]. The pantograph and the inter-coach gaps are typical aerodynamic noise source in high-speed trains.

Rolling noise is generated by the interaction between the wheels and the track, depending on their roughness [7]. An irregular wheel profile and a rail surface with irregularities generate higher levels of rolling noise than even homogeneous surfaces.

Separating the aerodynamic and rolling noise contributions in a pass-by is a challenging task [8]. A typical approach

* *anaelisa.alvesvieira@talgo.com*

consists in combining measurements and simulations. The aerodynamic noise sources can be assessed through microphones array measurements, using beamforming techniques [9]. The software TWINS (Track Wheel Interaction Noise Software) [10] is widely used to calculate rolling noise, as the wheel and track components are usually determined using simulations.

Aerodynamic noise generation mechanisms are currently well understood due to extensive wind tunnel measurements, field measurements and simulations performed over the last 20 years of research [11]. Researchers found that the ranking of the dominant aerodynamic noise sources changes depending on the train configuration. Therefore, reducing pass-by noise requires identifying the dominant noise sources during the design phase of a new train, which is usually done through simulations, as testing scale models in a wind tunnel is expensive and not always feasible.

Talgo's unique running gear, *rodal*, impacts both aerodynamic and rolling noise. Figure 1 shows a typical running gear configuration of Talgo high-speed trains.

A *rodal* has a smaller contact surface with the track than a bogie, since it has two wheels instead of four. Consequently, a lower value of rolling noise is expected for the *rodal* than for a bogie.

Figure 1. Inter-coach gap with a *rodal*.

The turbulent flow in the inter-coach gap is also affected by the *rodal*. In a design with bogies, the wheels are under the coach, but in the *rodal* the wheels are located in-between coaches. The different location and number wheels of the running gear have an impact on the turbulent field around the inter-coach area, which means that the aerodynamic noise contribution of a *rodal* and a bogie are different.

This research work aims to simulate the aerodynamic noise generated by an inter-coach gap with a *rodal*. As to the best of the author's knowledge, this type of analysis has only been performed for inter-coach configurations with a bogie.

Aerodynamic noise can be calculated using different approaches. In the railway industry, aeroacoustic calculations are particularly challenging due to the large dimensions of a train and its components, such as the pantograph and the bogies.

In the direct noise computation (DNC) method, the aerodynamic and acoustic fields are computed simultaneously. The main advantage of this method is its accuracy, but the computational resources and the time required for the calculation [12] make this method unsuitable for the case analyzed in this work.

An alternative to the DNC method is a hybrid approach [13]. This method uses an acoustic analogy (such as the Lighthill's or the Ffowcs-Williams Hawkings analogies) to determine the noise source, using the velocity and pressure fields calculated through a computational fluid dynamics (CFD) simulation. The noise source is then propagated to far-field observer positions.

Semi-empirical methods [14] and the Stochastic Noise Generation and Radiation (SNGR) method [15] are a valid option to obtain fast estimates and to perform comparative analysis. However, those approaches are not as flexible and accurate as DNC and hybrid methods.

This research work uses a hybrid approach to calculate the aerodynamic noise generated by an inter-coach gap, combining a Large Eddy Simulation (LES) [16] with the Lighthill's analogy [17].

The CFD method applied in this work is described in Section 2, and a description of the aeroacoustic simulation is given in Section 3. Section 4 shows the obtained results and how they correlate with measurements. Finally, Section 5 summarizes the main results and conclusions of this work.

2. CFD SIMULATION

The CFD simulation was performed using Hexagon's software Cradle [18]. The mesh was generated using the voxel fitting feature of the preprocessor. This meshing approach builds a voxel mesh directly from the geometry (either CAD or facetted data) and inserts a prism-layer after the volume mesh generation. This meshing process reduces both meshing and computation time.

This work aims to simulate the aerodynamic noise generated by a middle inter-coach gap (the airflow in the first and last inter-coach gaps has a different behavior due to the influence of the head, tail, and pantograph). Analyzing the entire train is computationally demanding, and the flow conditions should therefore be approximated. In the simplified train geometry used in this work, the inter-coach is placed at a 38m distance from the head. The head is followed by a simplified clean surface until the inter-coach gap position to minimize the number of mesh elements.

These simplifications aim to approximate the airflow in a middle inter-coach gap without simulating the complete train. The presence of the head in the geometry assures a realistic transition from laminar to turbulent flow, and the clean surface between the head and the inter-coach gap approximates the mid-train airflow condition. Figure 2 shows the geometry simplifications and the inter-coach position

relative to the train head. The inter-coach gap geometry presents a high level of detail.
The volume domain used in the CFD analysis has a length of 65*m*, a width of 33*m* and a height of 11*m*. An auxiliar domain was created to export the CFD results to the aeroacoustic simulation. This auxiliar domain, defined in the location of the inter-coach gap, has a length of 15*m*, a width of 7*m* and a height of 6.5*m*.

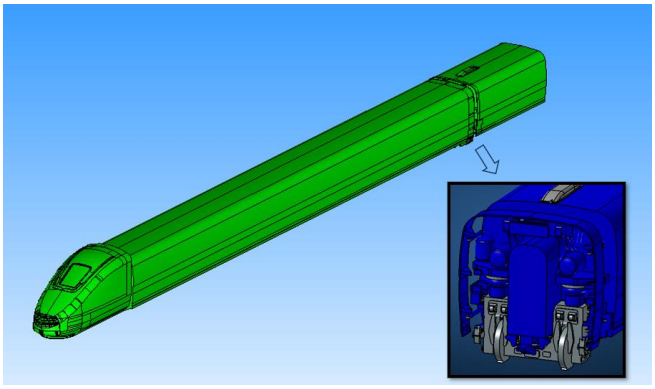

Figure 2. Geometry used to model the airflow in the inter-coach gap.

The volume mesh has 4 layers of 1cm elements, and the growing rate was defined as 2. This resulted in a model of 75M of elements. The geometry seems to be well-defined with this mesh refinement, as observed in Figure 3.

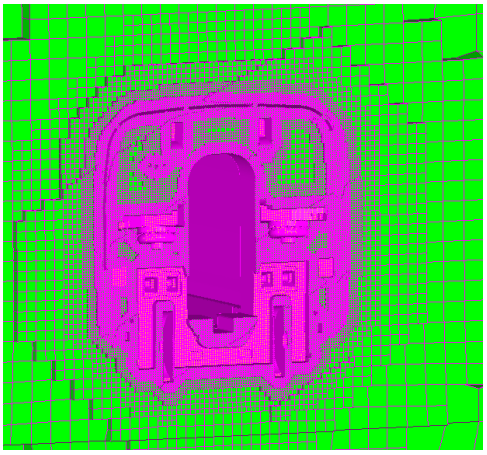

Figure 3. Mesh refinement in the inter-coach gap.

The analysis considered a train velocity of 280 km/h, i.e., the airflow can be considered as incompressible.
The initial conditions of the flow were obtained using a Reynolds-Averaged Navier-Stokes (RANS) model. Those initial conditions were then used as input in the transient analysis.
In the transient analysis, the turbulent flow was modelled using a Large Eddy Simulation (LES), with a time step of 3.75e-5 seconds. The velocity field of the auxiliary domain was saved every 1e-4 seconds. The total time of the CFD analysis was 0.1 seconds.
The computational time was approximately 72 hours, in a CPU with 48 cores, 512 GB RAM and 2 processors Intel(R) Xeon(R) Gold 6248R @ 3GHz 2.99 GHz.

3. AEROACOUSTIC SIMULATION

The aeroacoustic simulation was performed using Actran [19]. The aeroacoustic sources were computed from the CFD data previously calculated with Cradle using the iCFD utility of Actran. For incompressible computation, the iCFD reads the velocity field in the time domain, averages the data, and interpolates it to the acoustic mesh in the frequency domain.
The frequency range of the aeroacoustic analysis is limited to 100-1600Hz due to the mesh size used in the CFD analysis and the time of 0.1 seconds of the simulation.
The aeroacoustic simulation aims to determine the noise generated by the inter-coach gap and *rodal* alone. Therefore, the geometry is defined as in Figure 4, where only the inter-coach gap, the *rodal*, and a small part of the adjacent coaches are considered.

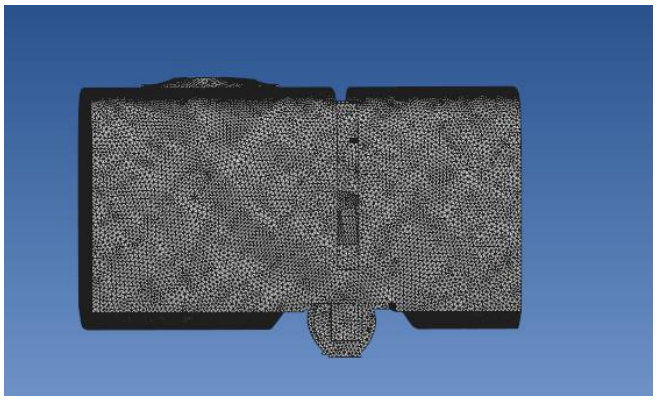

Figure 4. Geometry of the inter-coach gap used in the aeroacoustic simulation.

The mesh refinement was changed depending on the frequency range to keep a reasonable computational time. Lower frequencies can be calculated with coarser meshes than high frequencies. On the other hand, low frequencies require larger domains than high frequencies for the noise source computation. Generating different acoustic meshes depending on the target frequency is useful to limit the number of mesh elements. The acoustic mesh should be coarser than the CFD mesh to assure a valid interpolation.
The aeroacoustic field was computed using Lighthill's analogy. The calculations were based on a Finite Elements Method (FEM) formulation.
Infinite elements with a non-reflective boundary were used to propagate the noise sources to the far-field. An observer position aligned with the inter-coach gap was defined at a 7.5*m* distance and a height of 1.2*m* from the track, as defined

by the ISO EN 3095: 2013"*Measurement of noise emitted by railbound vehicles*".
The frequency resolution of the simulation was of 25 Hz. The computational time was different depending on the mesh refinement. The iCFD computation was of approximately 1h for low frequencies, increasing up to 5h for the highest frequencies. The aeroacoustic FEM computation was approximately 1h per frequency step for low frequencies, up to 5h per frequency step for the highest frequencies. The aeroacoustic simulation was performed in the same CPU as the CFD simulation.

4. RESULTS

This section shows the results obtained for the CFD and aeroacoustic simulations. Figure 5 shows the velocity field in the inter-coach gap. The highest values of velocity are located at the bottom part of the coach where there is more interaction between the airflow and the *rodal*.

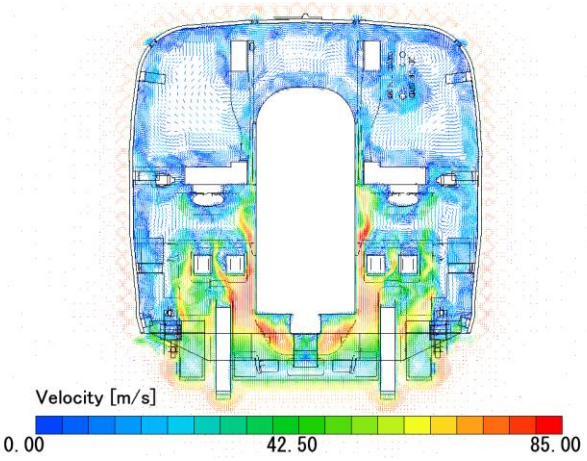

Figure 5. Velocity field calculated in the CFD analysis.

Figure 6 and Figure 7 show the aerodynamic noise contours around the inter-coach gap in dBA, at the frequency of 400 Hz.

The color scale of the noise plots is not presented for confidentiality of the results. The red and blue colors indicate maximum and minimum values, respectively. Higher levels of noise are observed close to the wheels and under the coach than in the middle of the inter-coach gap.

The noise contour at high frequencies has a similar distribution as in low frequencies, as shown in Figure 8 and Figure 9, for the frequency of 800 Hz. There are no significant noise sources generated at the top of the inter-coach gap, the highest values of noise are around the wheels and under the coach.

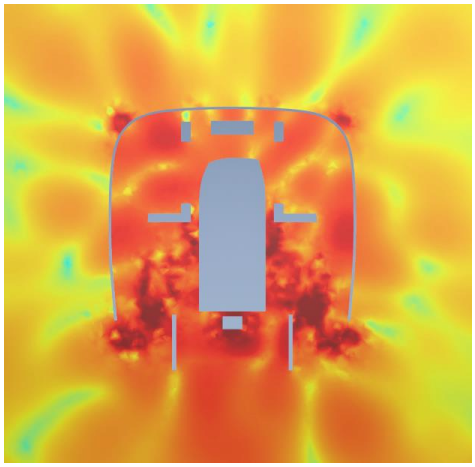

Figure 6. Aerodynamic noise generated at the inter-coach gap at the frequency of 400 Hz (front view).

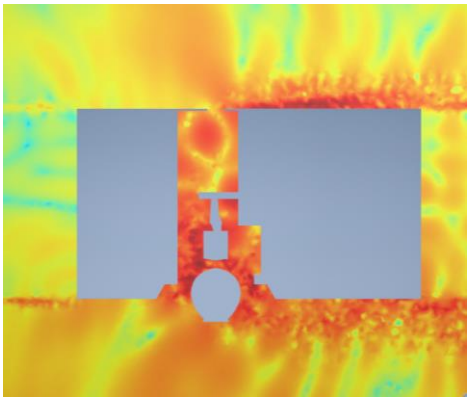

Figure 7. Aerodynamic noise generated at the inter-coach gap at the frequency of 400 Hz (side view).

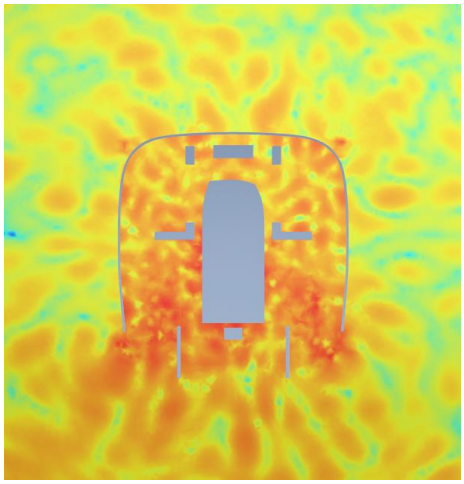

Figure 8. Aerodynamic noise generated at the inter-coach gap at the frequency of 800 Hz (front view).

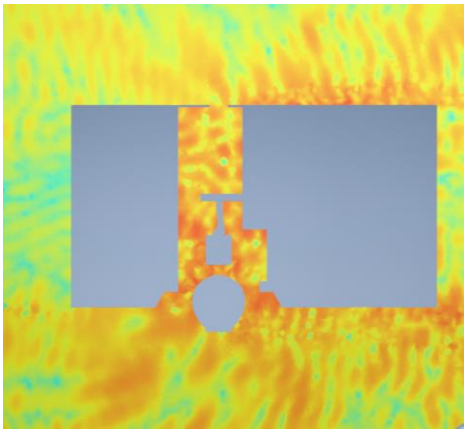

Figure 9. Aerodynamic noise generated at the inter-coach gap at the frequency of 800 Hz (side view).

Figure 10 shows the A-weighted spectrum calculated for an observer position equivalent to a pass-by certification point. The spectrum is plotted in 1/3-octave bands.

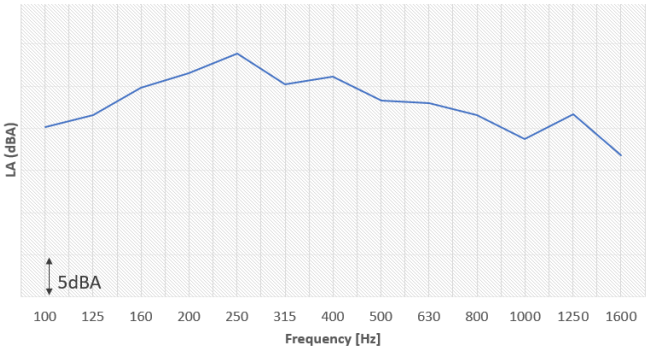

Figure 10. Normalized A-weighted noise spectrum calculated at a certification position (in 1/3-octave bands).

The spectrum is approximately constant over the mid-frequency range, showing a peak at 250Hz. The noise level slightly decreases for frequencies higher than 1000 Hz. This decrease can indicate that the mesh used in the CFD computation should be further refined. A convergence analysis (varying the refinement of the CFD and acoustic meshes) is the best option to verify if this decrease of the spectrum at high frequencies is due to mesh parameters. However, that is not feasible in the case of the inter-coach gap due to the large computational time.

The A-weighted overall sound pressure level (OASPL) of the aerodynamic noise generated by the inter-coach gap noise was obtained from the spectrum of Figure 10 and compared with pass-by measurements of a Talgo's high-speed train at the velocity of 280 km/h. Figure 11 shows two pass-by curves measured at the high-speed track Madrid-Barcelona (black and gray curves) together with the OASPL value calculated for the aerodynamic noise generated by the inter-coach gap (red curve). The frequency range of the experimental pass-by curve was limited to 100-1600Hz, as in the simulation.

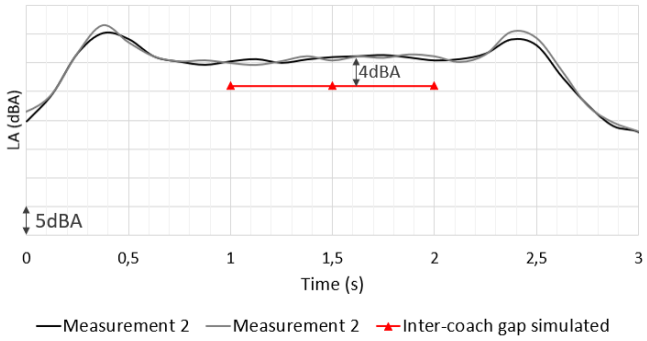

Figure 11. Normalized pass-by curves of a Talgo's high-speed train at the velocity of 280 km/h, measured at the certification point (7.5*m* distance and 1.2*m* height from the track) considering a 100-1600Hz frequency range.

In this train configuration, the traction and ventilation systems are all located in the powerheads (head and tail of the train). Therefore, the maximum values of the pass-by curve, correspond to the powerheads. The noise values at the middle of the curve are a result of the aerodynamic and rolling noise generated at the inter-coach gap/*rodal*. All coaches have HVAC (heating, ventilation, and air conditioning) system units but they are negligible noise sources to the pass-by noise.

The difference of noise level between the experimental pass-by curve at the coach locations and the value calculated for the aerodynamic noise at the inter-coach gap is 4 dBA.

At the speed of 300 km/h, the contribution of the aerodynamic and rolling noise is estimated to be approximately the same according to literature [20]. This means that the aerodynamic noise contribution is expected to be 3dBA below the total pass-by noise curve. In the case analyzed in this work, the operating velocity is slightly below 300 km/h and therefore the rolling noise contribution to total noise is expected to be slightly higher than the aerodynamic noise contribution. The OASPL value calculated for the aerodynamic noise generated by the inter-coach gap can therefore be considered realistic.

5. CONCLUSIONS

This work determined the aerodynamic noise contribution of an inter-coach gap with a *rodal* to the pass-by noise of a Talgo's high-speed train.

The computational method applied was based on a hybrid approach. The operational velocity of the train was 280 *km/h*, which means that the flow can be considered as uncompressible. The velocity field in the inter-coach gap was calculated with a LES. This output was used in the aeroacoustic simulation to determine the noise sources, using the Lighthill's analogy. The near-field results are then propagated to the far-field (up to an observer position

equivalent to a certification point of a pass-by) using infinite elements.

The CFD results show higher velocity values around the wheels and below the coaches than in the top region of the inter-coach gap. The aeroacoustic analysis shows that those are the regions where the highest values of aerodynamic noise are generated.

The spectrum calculated at the certification point shows a peak at the 1/3-octave band of 250 Hz. The spectrum decreases slightly for higher frequencies, which can indicate that the CFD mesh needs to be further refined.

Nevertheless, the overall value (considering a frequency range of 100-1600Hz) determined for the aerodynamic noise generated at the inter-coach gap seems realistic when compared to experimental results.

Future work should focus on the accuracy of the results at high frequencies and on the comparison of the calculated spectrum with an experimental spectrum determined using noise source separation methods.

6. REFERENCES

[1] E. Bachman, A. Tavasoli, T. A. Hatton, C. T. Maravelias, E. Haites, P. Styring, A. Aspuru-Guzik, J. MacIntosh and G. Ozin, "Rail-based direct air carbon capture," *Joule*, 2022.

[2] R. Barcikowska and E. Wawrzyn, "Selected Sources of Research Funding in Railway Transport," *WUT Journal of Transportation Engineering*, vol. 136, pp. 85-99, 2023.

[3] A. Seidler, M. Schubert, Y. Mehrjerdian, K. Krapf, C. Popp, I. v. Kamp and J. H. Mikael Ögren, "Health effects of railway-induced vibration combined with railway noise – A systematic review with exposure-effect curves," *Environmental Research* , vol. 233, 2023.

[4] R. Pieren, F. Georgiou, G. Squicciarini and D. Thompson, "Auralisation of combined mitigation measures in railway pass-by noise," in *InterNoise*, Glasgow, UK, 2022.

[5] E. C. Talotte, "Aerodynamic Noise: A Critical Survey," *Journal of Sound and Vibration*, vol. 231, no. 3, pp. 549-562, 2000.

[6] F. Shi, F. Shi, X. Tian and T. Wang, "Numerical Study on Aerodynamic Noise Reduction of Pantograph," *Applied Sciences*, vol. 12, no. 21, 2022.

[7] X. Garcia-Andrés, J. Gutiérrez-Gil, J. Martínez-Casas and F. D. Denia, "Wheel shape optimization approaches to reduce railway rolling noise," *Structural and Multidisciplinary Optimization* , vol. 62, p. 2555–2570, 2020.

[8] E. Verheijen, "Using source separation techniques in measuring," in *Inter-Noise*, Prague, 2004.

[9] E. Sarradj, C. Schulze and A. Zeibig, "Aspects of source separation in beamforming," in *BeBeC*, Berlin, 2006.

[10] C. Talotte, "Railway source models for integration in the new European noise prediction method proposed in Harmonoise," *Journal of Sound and Vibration*, vol. 293, p. 975–985, 2006.

[11] X.-M. Tan, H.-f. Liu, Z.-G. Yang, J. Zhang, Z.-g. Wang and Y.-w. Wu, "Characteristics and Mechanism Analysis of Aerodynamic Noise Sources for High-Speed Train in Tunnel," *Complexity*, 2018.

[12] J. Friedrich and M. Schafer, "Acoustics Simulation in the Presence of Moving Interfaces in Multiphase Flows," in *6th European Conference on Computational Mechanics*, Glasgow, 2018.

[13] S. Schoder and M. Kaltenbacher, "Hybrid Aeroacoustic Computations: State of Art and New Achievements," *Journal of Theoretical and Computational Acoustics*, vol. 27, no. 9, 2020.

[14] E. Latorre Iglesias, D.J.Thompson and M.G.Smith, "Component-based model to predict aerodynamic noise," *Journal of Sound and Vibration*, vol. 394, pp. 280-305, 2017.

[15] B. d. Brye, A. Poulos, C. Legendre and G. Lielens, "A cost-effective computational technique for aeroacoustic," in *ISMA 2020 Conference*, 2020.

[16] J. Ferziger, "Large Eddy Simulation: An Introduction and Perspective," in *New Tools in Turbulence Modelling. Centre de Physique des Houches*, Berlin, 1997.

[17] S. Caro, P. Ploumhans and X. Gallez, "Implementation of Lighthill's Acoustic Analogy in a Finite/Infinite Elements Framework," in *10th AIAA/CEAS Aeroacoustics Conference*, Belgium, 2004.

[18] HEXAGON, "Cradle CFD Version 2021 Release Notes," 2021.

[19] HEXAGON, "Actran 2022 - User's Guide ActranVI," 2022.

[20] E. Masson, N. Paradot and E. Allain, "The Numerical Prediction of the Aerodynamic Noise of the TGV POS High-Speed Train Power Car," in *Noise and Vibration Mitigation for Rail Transportation Systems* , 2012.